

ARTICLE

Microfibers nanocomposite based on polyacrylonitrile fibers/bismuth oxide nanoparticles as X-ray shielding material

Mehdi Rashidi¹ | Aram Rezaei¹  | Salar Bijari² | Mehdi Jaymand¹ | Hadi Samadian¹ | Elham Arkan¹ | Saleh Salehi Zahabi^{3,4} | Mehdi Hosseini⁵

¹Nano Drug Delivery Research Center, Health Technology Institute, Kermanshah University of Medical Sciences, Kermanshah, Iran

²Department of Medical Physics, Faculty of Medical Sciences, Tarbiat Modares University, Tehran, Iran

³Radiology and Nuclear Medicine Department, School of paramedical, Kermanshah University of Medical Sciences, Kermanshah, Iran

⁴Clinical Research Development Center, Taleghani and Imam Ali Hospitals, Kermanshah University of Medical Sciences, Kermanshah, Iran

⁵Department of Chemistry, Faculty of Basic Science, Ayatollah Boroujerdi University, Boroujerd, Iran

Correspondence

Aram Rezaei and Hadi Samadian, Nano Drug Delivery Research Center, Health Technology Institute, Kermanshah University of Medical Sciences, Kermanshah, Iran.

Email: aram.rezaei@gmail.com; aram.rezaei@kums.ac.ir (A. R.) and h30samadian@gmail.com (H. S.)

Funding information

Kermanshah University of Medical Sciences, Grant/Award Number: 97052

Abstract

The main focus of the current study was to fabricate fibrous nanocomposite based on polyacrylonitrile (PAN) fibers containing Bi₂O₃ NPs as the X-ray shielding material. Bi₂O₃ NPs were synthesized based on the solid dispersion evaporation method and dispersed into PAN polymer solution with different weight concentrations. The electrospinning technique was used to fabricate nanocomposite. The morphology, surface functional group, wettability, elemental analysis, and X-ray shielding efficacy of the fabricated nanocomposite were thoroughly evaluated. The diameter of the fibrous nanocomposites containing 10, 20, and 30 wt% Bi₂O₃ NPs were 1.33 ± 0.08, 1.01 ± 0.11, and 1.69 ± 0.32 μm, respectively. EDX elemental analysis showed that NPs were uniformly distributed into/onto the fibers. The X-ray shielding studies showed that the prepared nanocomposites effectively attenuate the intensity of the X-ray. The entrance surface dose for the negative control was 24.10 ± 1.71 mSv and the application of the nanocomposites significantly reduced the entrance surface dose. The results showed NPs concentration-dependent CT number shift as the indication of X-ray protection and the highest value was obtained by 30 wt% NPs. The obtained results implied that the fabricated nanocomposites effectively attenuate the radiation and they could be applied as the X-ray shielding materials.

KEYWORDS

applications, biomedical applications, composites, nanoparticles, nanowires and nanocrystals, X-ray

1 | INTRODUCTION

X-ray applications have been expanding in various fields of medicine, the food industry, agriculture, space exploration, generating electricity, and archaeology (carbon dating).^{1,2} Moreover, X-ray-based medical diagnosis and treatment methods are widely applied in different diseases. Despite its

beneficial impact on the fields, the hazardous effects of X-ray on the human body are documented and it is reported that medical diagnostic X-ray examinations cause more than 80% of public exposure.^{3–5} Accordingly, unprecedented attempts have been conducting to develop efficient shielding materials protecting patients and the public from unwanted X-ray exposure. Conventionally, lead (Pb)-based structures have

been applying as the shielding materials. Despite the superb shielding efficacy of Pb-based shielding structures, significant toxicity and ecotoxicity concerns have been raised on these materials.^{6–8} Therefore, unprecedented studies have been conducted to develop efficient, non-toxic, and more eco-friendly shielding materials.

Nanomaterials and nanotechnology as the enabling approaches have promising effects on the conventional structures and processes.^{9–11} Nanomaterials exhibit altered and modified performance compared with the bulk counterparts.^{12–15} Moreover, it is possible to modify the properties and performance of conventional materials and structures modified by the implementation of nanomaterials.^{11,16–19} NPs synthesized from high Z materials, such as gold NPs, exhibit X-ray attenuating performance. Despite its shielding efficacy and biocompatibility, but its high cost prevents its use in real.^{20,21} Alternatively, bismuth (Bi)-based NPs could be applied due to their high X-ray attenuation coefficient. Bi-based NPs offer biocompatibility, X-ray sensitive capabilities, well-established chemistry, near-infrared driven semiconductor properties, and low-cost production process.²² The positive effects of Bi on the treatment of syphilis, hypertension, stomach ulcers, infections, gastrointestinal disorders, and skin conditions have been reported.^{23,24} Since Bi NPs are not self-standing, they must be embedded into or onto a proper matrix. Various types of structures such as fabrics, ointment and nanofibers could be applied as the holding matrix.

Nanofibers are fascinating nanostructures with promising applications in various filed from medicine to different industries. They are prepared from different natural, synthetic and semi-synthetic polymers by the electrospinning technique.^{25,26} Electrospinning is a versatile, flexible, high throughput, and simple nanofiber production method. Various environmental and system parameters are involved and influenced by these methods, enabling us to manipulate the parameters and produce the desired nanofibers with different compositions, morphologies, and architectures. Using the electrospinning technique, it is possible to fabricate nanofibrous nanocomposite containing different NPs.²⁷ Accordingly, in the present study, we aimed to combine the X-ray shielding property of Bi oxide NPs with polyacrylonitrile (PAN) fibers. To the best of our knowledge, the prepared nanocomposites are novel structures with promising potential as the X-ray shielding construct.

2 | MATERIALS AND METHODS

2.1 | Materials

PAN (MW: 80,000 g/mol) was obtained from Polyacryl Company (Iran). Bismuth(III) nitrate pentahydrate (Bi

(NO₃)₃·5H₂O) (98% in purity) and sorbitol 70% were purchased from Sigma-Aldrich (St. Louis MO, USA). Dimethylformamide (DMF) was obtained from Merck (Darmstadt, Germany).

2.2 | Nanoparticles synthesis

The bismuth oxide nanoparticles were synthesized based on the solid dispersion evaporation technique.²⁸ Briefly, Bi(NO₃)₃·5H₂O (5 g) was dissolved in a mixture solution of sorbitol (0.717 ml) and deionized (DI) water (1.43 ml), stirred for 24 h at room temperature and sonicated for 30 min at 25°C (37 kHz and 100 W) using a water bath sonicator (Elmasonic S100H, Germany). In this process, sorbitol acts as the reaction media along with DI. The solvent of the prepared solution was evaporated at 100°C for 30 min in a heating oven (Memmert, Germany). The resulted sample was decomposed at 400–450°C for 1 h.

2.3 | Fibrous nanocomposites synthesis

The synthesized NPs were dispersed in PAN polymeric solution and converted to the nanocomposite by electrospinning method. Briefly, three different concentrations of the synthesized NPs (0.1, 0.2, and 0.3 g) was added to 4 g DMF, stirred for 48 h at room temperature, sonicated three times for 20 min each run at 60°C. The resulted dispersion was further sonicated using a probe sonicator (ATHENA, ATP-750, INDIA) for 5 min in 60–64 W. In the next step, 1 g of PAN polymer was added to each dispersion and on stirrer for 72 h at room temperature to obtain 20 wt% PAN/DMF solution containing different concentrations of the NPs. The prepared solutions were loaded into a 5 ml syringe and converted to fibers using an electrospinning system with the following electrospinning parameters: the polymer solution feeding rate of 1 ml/min, nozzle to collector distance of 10 cm and applied voltage of 20 kV.

2.4 | Characterizations

The size of the synthesized NPs was measured based on the dynamic light scattering (DLS) method using a scateroscope (Malvern 4700, Malvern Instruments). The fibers' morphology was observed using scanning electron microscopy (SEM, FEI, quanta 450, USA). The nanocomposites were sputter coated with a thin layer of gold using a sputter coater (SCD 004, Balzers, Germany and imaged 20 kV accelerating voltage. Image J

(1.47v, National Institute of Health, USA) software was used to measure the fibers' diameter with measuring diameter of 20 fibers. Semi-quantitative elemental analysis was conducted using an EDX detector-equipped SEM system.

2.5 | Fourier transform infrared spectroscopy

Fourier transform infrared (FTIR) spectroscopy was conducted to assess the surface functional groups of NPs, the nanocomposites, and their possible interactions. The samples were prepared in pellet form with KBr powder and an experiment conducted using a Shimadzu 8101 M FTIR (Kyoto, Japan) at room temperature. The spectra were recorded at a wavenumber resolution of 4 cm^{-1} in a spectral range from 400 to 4000 cm^{-1} .

2.6 | Mechanical properties measurement

Mechanical properties of shielding structures have vital role in its implementation and shielding efficacy. The tensile strength of the prepared nanocomposites was measured using a uniaxial tensile testing device (Santam, Karaj, Iran) according to the ISO 5270:1999 standard test methods at a strain rate of 1 mm/min.

2.7 | Wettability assessment

Wettability characteristic of a shielding material has determinant role. The sessile droplet contact angle method was conducted to measure the wettability of the prepared fibers using a static contact angle measuring device (KRUSS, Hamburg, Germany).

2.8 | X-ray absorption studies

The X-ray absorption studies were conducted using a 16 slice spiral CT Scan (Toshiba Aquilion Series. The surface dose at the entrance of phantom was measured using LiF: Mg, Cu, P (GR200A) thermoluminescence dosimeters (TLD) by applying a poly(methyl methacrylate) tissue-equivalent phantom (diameter of 32 cm and a length of 15 cm) (Figure 1). Two critical parameters in CT scan procedure, the shield-induced dose reduction and image artifact, were evaluated by the clinically

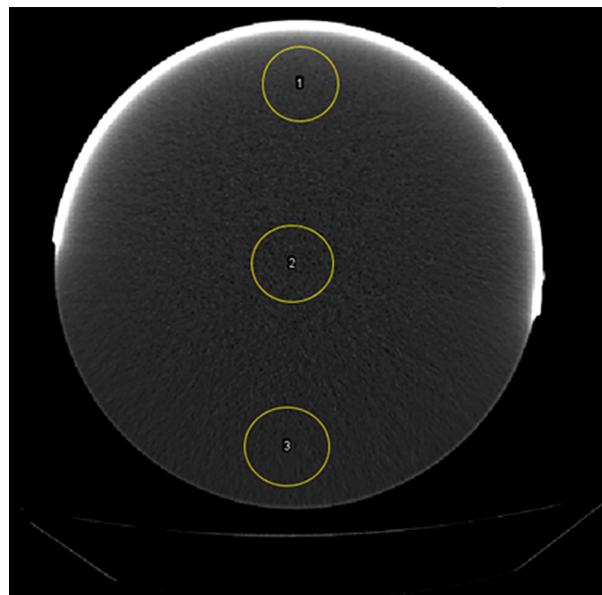


FIGURE 1 The X-ray absorption image [Color figure can be viewed at wileyonlinelibrary.com]

routine protocol of adult chest CT include 110 kVp, 150 MAS, 0.5 S rotation time, 1.5 pitch, and 5 mm slice thickness with common Reconstruction model in The THOSHIBA of software.

A calibrated TLD was used to measure the dose reduction by placing TLD dosimeter under the shield, four TLD of them above and on the right side, and others at the phantom's left side. The CT number shift (Hounsfield CT number of CT images) and percentage of noise increase (standard deviation of CT images) were measured as the function of shielding efficacy and artifact induction, respectively. These parameters were measured in five slice of images, at three different regions of interest (RIO) by placing the fabricated nanocomposites shields at four different distances away from the phantom, 0, 2, 4, and 6 cm. The images obtained from the phantom were analyzed with respect to the image noise and the CT using Image J (1.47v, National Institute of Health, USA) software at different ROIs.

2.9 | Statistical analysis

The statistical analysis was performed using the SPSS program, v.23 (IBM, Armonk, NY, USA) by applying a one-way ANOVA test with Tukey's multiple comparison test ($p < .05$). All experiments were conducted in triplicate, except the animal studies performed on six rats in each group. The results were reported as a mean \pm SD, and $p < .05$ was considered statistically significant.

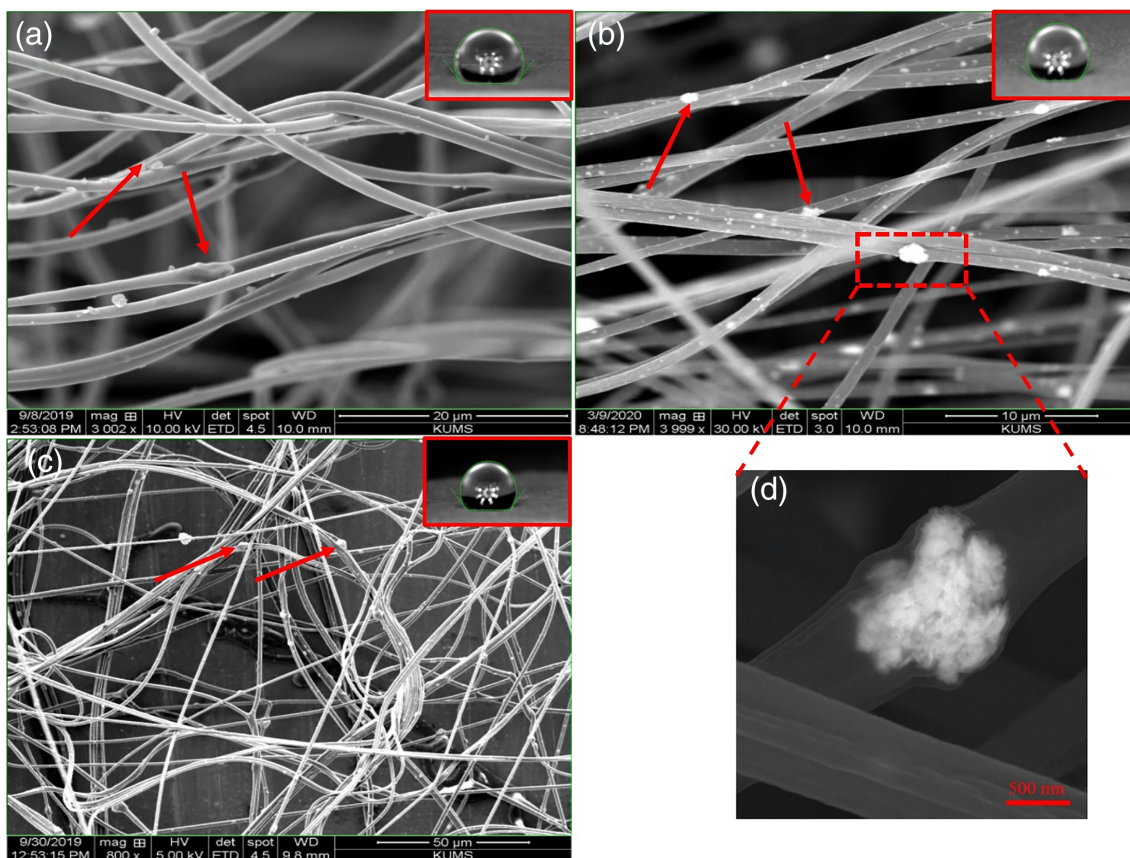


FIGURE 2 Scanning electron microscopy (SEM) micrograph of the nanocomposites. (a) PAN/Bi₂O₃ 10%, (b) PAN/Bi₂O₃ 20%, (c) PAN/Bi₂O₃ 30%, and (d) magnified image of Bi₂O₃ NPs-laden PAN fibers. Arrows: Bi₂O₃ NPs. The inserts: Wettability results [Color figure can be viewed at wileyonlinelibrary.com]

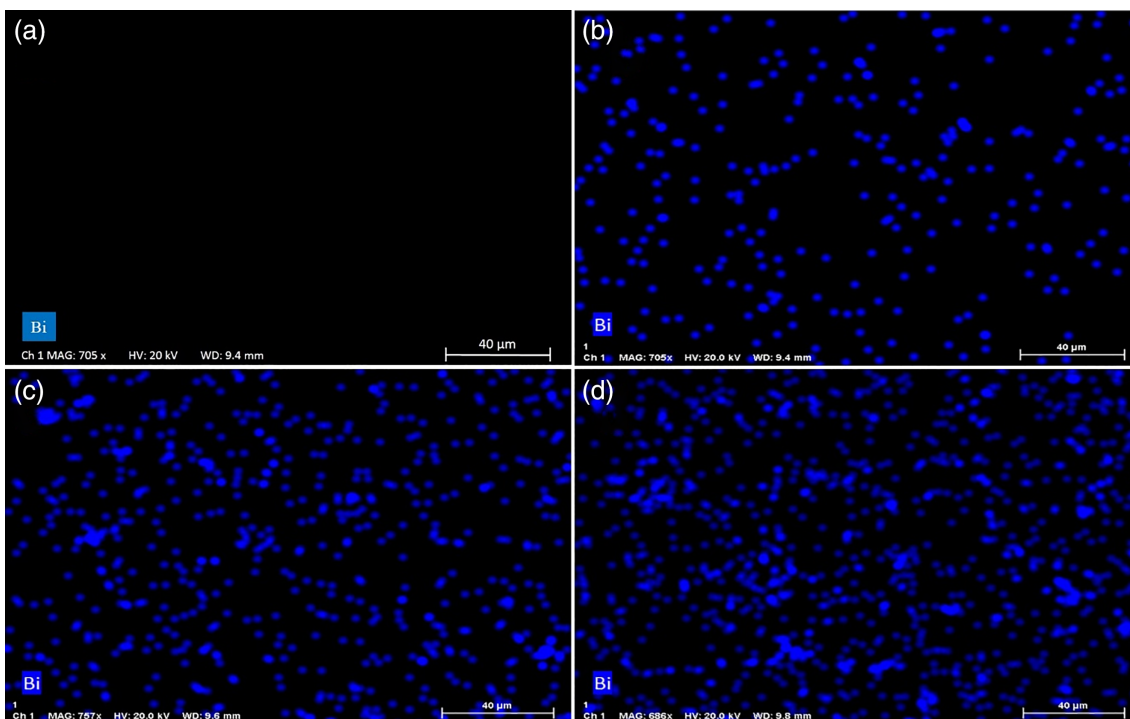


FIGURE 3 EDX map image of Bi in nanocomposites (a) PAN, (b) PAN/Bi₂O₃ 10%, (c) PAN/Bi₂O₃ 20%, and (d) PAN/Bi₂O₃ 30% [Color figure can be viewed at wileyonlinelibrary.com]

3 | RESULTS AND DISCUSSION

3.1 | Characterization results

The DLS results showed that the average diameter of the synthesized NPs was 100 nm with the polydispersity index (PDI) value of 0.428. Since the Bi_2O_3 NPs were synthesized based on the solid dispersion evaporation

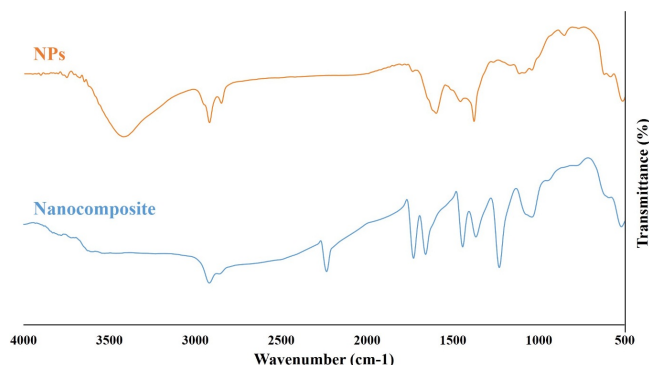


FIGURE 4 Fourier transform infrared (FTIR) spectra of Bi_2O_3 NPs and PAN/ Bi_2O_3 NPs [Color figure can be viewed at wileyonlinelibrary.com]

technique, its size measurement critically depends on the sample preparation before the measurement, such as proper sonication. The obtained size of NPs is desired for the intended application, since reducing the size of particles below 100 exponentially increases the surface area. Moreover, the obtained PDI indicates that the synthesized NPs are partially monodispersed. The morphology of the prepared nanocomposites was observed using SEM and the results are present in Figure 2. The fibers were uniform, straight, and beadless. The results showed that the diameter of PAN/ Bi_2O_3 10%, PAN/ Bi_2O_3 20%, and PAN/ Bi_2O_3 30% were 1.33 ± 0.08 , 1.01 ± 0.11 , and 1.69 ± 0.32 μm , respectively.

The presence of Bi_2O_3 NPs into/onto the nanocomposites (Figure 2, arrows) was shown in the SEM images and EDX analysis (Figure 3). These findings revealed that the synthesized Bi_2O_3 NPs were properly dispersed throughout the nanofibrous shield. The wettability of the nanocomposites was evaluated based water contact angle method and the results are presented in as inserts in Figure 2. The results showed that the water contact value for PAN/ Bi_2O_3 10%, PAN/ Bi_2O_3 20%, and PAN/ Bi_2O_3 30% were 126 ± 5 , 130 ± 7 , and $128 \pm 4^\circ$, respectively. The results showed that

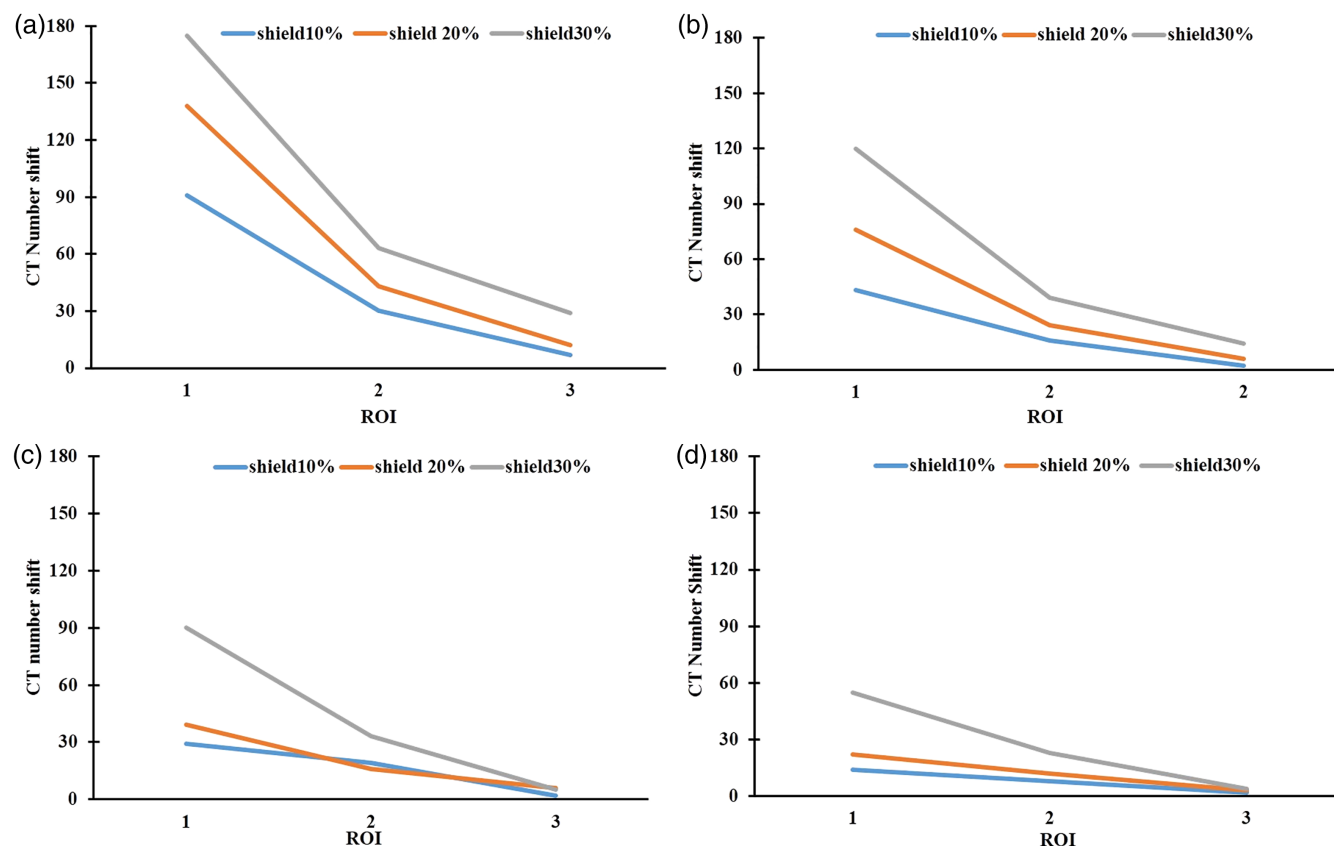


FIGURE 5 The effect of the prepared nanocomposite shields on the CT number shift at the different distances between the shields and the phantom. (a) 0, (b) 2, (c) 4, and (d) 6 cm [Color figure can be viewed at wileyonlinelibrary.com]

increasing the concentration of the NPs did not significantly change the water contact value of the nanocomposites ($p < .2$). The obtained results imply that the prepared nanocomposites possess hydrophobic, which is beneficial for the future applications of the prepared fibers as waterproof wearable shields.

EDX elemental analysis was performed to further evaluate the presence of Bi_2O_3 NPs and the results of the EDX map for the Bi element are presented in Figure 3. The results confirmed the presence of Bi_2O_3 NPs into/onto the nanocomposites and the differences are apparent within the groups. There are not any signs of Bi_2O_3 NPs in pure PAN fibers appeared in Bi_2O_3 NPs containing groups.

The surface functional groups on the synthesized Bi_2O_3 NPs and the prepared nanocomposite was detected using FTIR spectroscopy (Figure 4). The characteristic peaks of PAN fibers are presented in Figure 4. The sharp peaks located at 2223 and 1658 cm^{-1} correspond to the nitrile group ($\text{C}\equiv\text{N}$). The peaks at 2938, 1453, 1357, and 1249 cm^{-1} are related to the vibrations of the aliphatic CH groups (CH , CH_2 , and CH_3). On the other hand, in NPs spectrum, the peaks located at 510–574 cm^{-1} correspond to Bi–O stretching vibrations and the peaks at

1076 and 1107 cm^{-1} correspond to C–OH groups. The peak located at 1454 and 1597 cm^{-1} are related to C–N and N–H, respectively. In the nanocomposite spectrum, the characteristic peaks of PAN and Bi_2O_3 NPs are presented. Moreover, the peak located at 1442 cm^{-1} is related to the deformation vibration of CH_2 . These observations confirmed the interactions of Bi_2O_3 NPs surface functional groups with PAN polymer.

3.2 | X-ray shielding findings

Measuring the entrance surface dose (ESD) through the nanocomposites and nanocomposites' effects on image noise and CT number during the chest CT scan were conducted to evaluate the shielding quality of the prepared nanofibers. ESD value for the negative control (exposure without shield) during chest CT scan was 24.10 ± 1.71 mSv, considered a 0% shielding effect. PAN fibers' application containing 10, 20, and 30% Bi_2O_3 NPs resulted in 38.2%, 46.8%, 52.6% shielding, respectively. These results showed that the application of Bi_2O_3 NPs significantly induced shielding effects ($p < .05$). EDS, as the amount of radiation dose to the patient, was

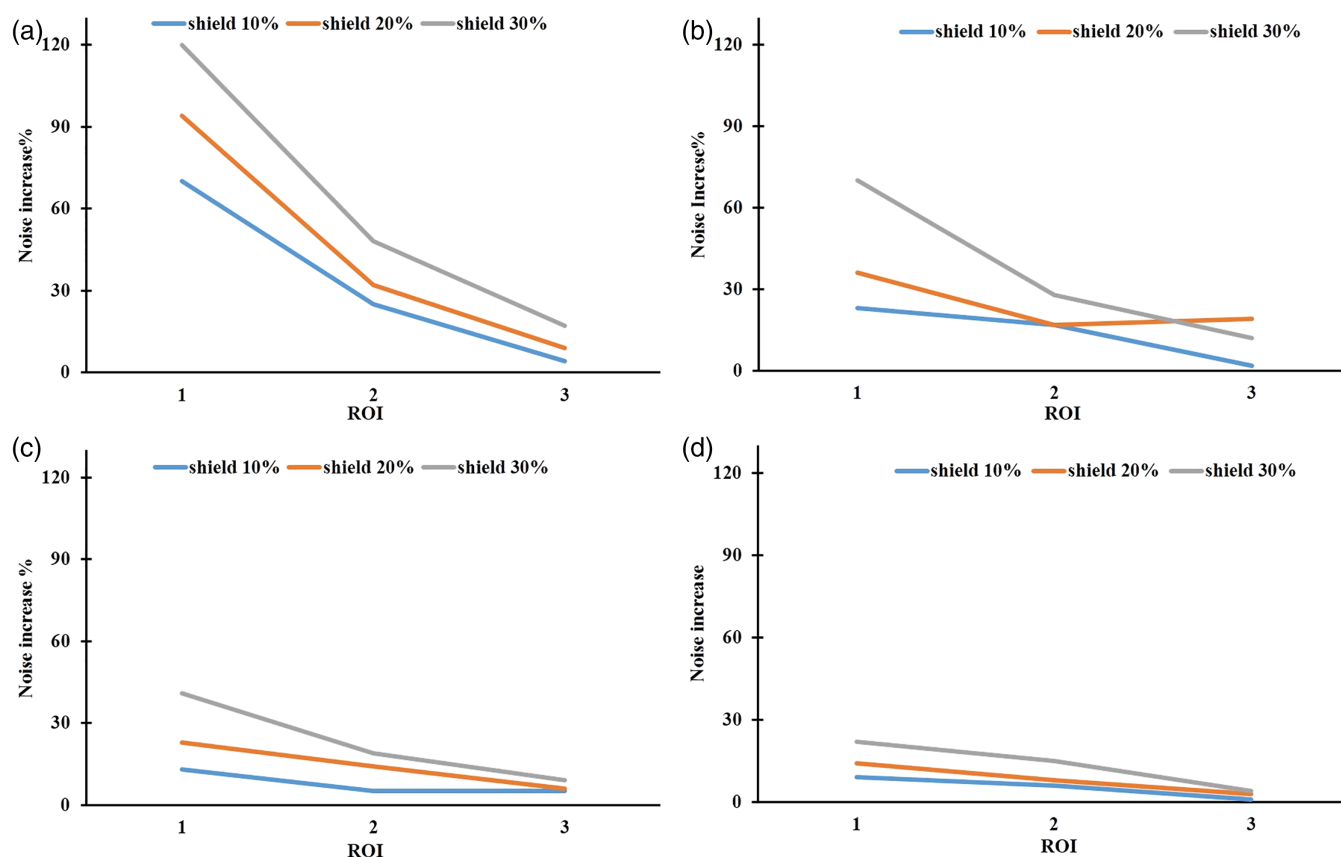


FIGURE 6 The effect of the prepared nanocomposites on the image noise at different distance between the shields and the phantom. (a) 0, (b) 2, (c) 4, and (d) 6 cm [Color figure can be viewed at wileyonlinelibrary.com]

measured to evaluate the shielding efficacy of the nanocomposites. The obtained results indicate that the incorporation of Bi_2O_3 NPs attenuate the EDS and exhibited promising shielding effect.

The CT number shifts under the administration of the prepared nanocomposite shields were measured as the function of the shielding effect. The prepared nanocomposite shields were placed at four different distances from the phantom, 0, 2, 4, and 6 cm, and the CT number shifts were measured at three different ROIs (Figure 5). The results showed that the nanocomposite shield containing 30% Bi_2O_3 NPs induced the highest CT number shift. These observations indicate that the highest concentration of Bi_2O_3 NPs could affect the CT number. Moreover, it was observed that increasing the distance between the nanocomposite shields and the applied phantom reduce the shielding artifact. This observation can be attributed to the X-ray scattering elimination induced by the nanocomposite shield.

In the CT scan, it is critical to balance the shielding effect and the induced artifact in the image. Accordingly, an optimum condition should be obtained between the highest shielding effect and the lowest artifact. The nose percent in the obtained images were measured as the shield-induced artifacts' function, and the results are presented in Figure 6. The results showed that the implementation of the nanocomposite shield containing 30% Bi_2O_3 NPs induced the highest noise. Moreover, it was observed that there is an inverse correlation between noise induction and distance from between the shields and the phantom.

These results showed that PAN/ Bi_2O_3 NPs nanocomposites' application improved the shielding effect in a concentration-dependent manner. These results are in good agreement with those of a previous report that reported the shielding effects on nanofibers containing bismuth NPs. Hazlan et al.²⁹ evaluated and compared X-ray attenuation efficacy of PVA/ Bi_2O_3 and PVA/ WO_3 nanocomposites. They reported that the PVA/ Bi_2O_3 nanocomposite was more effective than PVA/ WO_3 nanocomposite. In another study, Ji et al.,³⁰ fabricated crosslinking PAN (CPAN) containing different NPs, Cu, Ni, and AgNPs, a flexible electrospun polymer nanofiber/metal nanoparticle hybrid membrane for high-performance electromagnetic interference shielding. They reported significant EMI shielding effectiveness by CPAN/AgNPs mat.

4 | CONCLUSION

The conventional lead-based X-ray shielding materials suffer from significant toxicity and ecological issues. With the advancements in chemistry and materials sciences,

especially nanomaterials, it is possible to fabricate shielding materials with improved shielding effects and lower toxicological issues. Accordingly, in the present paper with fabricated fibrous shielding materials based on PAN microfibers containing different concentrations of Bi_2O_3 NPs. The results showed that the synthesized NPs were monodisperse and in the size lower than 100 nm. The nanofibers characterization implied that the NPs are appropriately dispersed throughout the PAN fibers and did not induce adverse effects on nanofibers' morphology. The X-ray shielding studies showed that the nanocomposites effectively attenuate X-ray and act as shielding materials. Although the implementation of the nanocomposite shield containing 30% Bi_2O_3 NPs induced the highest X-ray protection, it also caused the highest noise in images, an adverse effect. By varying the distance between the nanocomposite and the target site (phantom or patient body), the highest protection and lowest artifact could be touched. This study implies that the PAN/ Bi_2O_3 nanocomposites can be applied as an efficient shielding material with the minimum toxicological concerns.

ACKNOWLEDGMENTS

We gratefully acknowledge the Research Council of Kermanshah University of Medical Sciences for providing the facilities and financial support for this work (Grant number 97052).

ORCID

Aram Rezaei  <https://orcid.org/0000-0003-2408-7254>

REFERENCES

- [1] S. Dabagov, Y. Gladkikh, *Radiat. Phys. Chem.* **2019**, *154*, 3.
- [2] D. Š. Jung, T. Donath, O. Magdysyuk, J. Bednarcik, *Powder Diffr.* **2017**, *32*, S22.
- [3] B. Bennett, *Radiat. Prot. Dosim.* **1991**, *36*, 237.
- [4] G. Marinskis, M. G. Bongiorno, N. Dages, T. Lewalter, L. Pison, C. Blomstrom-Lundqvist, conducted by the Scientific Initiative Committee, E. H. R. A, *Europace* **2013**, *15*, 444.
- [5] A. Stewart, G. W. Kneale, *Lancet* **1970**, *295*, 1185.
- [6] P. Limkitjaroenporn, J. Kaewkhao, P. Limsuwan, W. Chewpraditkul, *J. Phys. Chem. Solids* **2011**, *72*, 245.
- [7] H. Fares, I. Jlassi, H. Elhouichet, M. Férid, *J. Non-crystalline Solids* **2014**, *396*, 1.
- [8] L. W. Klein, D. L. Miller, S. Balter, W. Laskey, D. Haines, A. Norbash, M. A. Mauro, J. A. Goldstein, *Radiology* **2009**, *250*, 538.
- [9] B. Massoumi, M. Abbasian, R. Jahanban-Esfahlan, S. Motamedi, H. Samadian, A. Rezaei, H. Derakhshankhah, A. Farnudiyan-Habibi, M. Jaymand, *Polym. Int.* **2020**, *69*, 519.
- [10] A. Ramazani, A. Rezaei, A. Mahyari, M. Rouhani, M. Khoobi, E. Yaaghubi, H. Shabrendi, E. Vessally, V. Azizkhani, I. Amini, *Synth. Commun.* **2011**, *41*, 1444.

- [11] A. Ramazani, Y. Ahmadi, N. Fattahi, H. Ahankar, M. Pakzad, H. Aghahosseini, A. Rezaei, S. T. Fardood, S. W. Joo, *Phosphorus Sulfur Silicon Relat. Elem.* **2016**, *191*, 1057.
- [12] L. Hadian-Dehkordi, A. Rezaei, A. Ramazani, M. Jaymand, H. Samadian, L. Zheng, X. Deng, H. Zheng, *ACS Appl. Mater. Interfaces* **2020**, *12*, 31360.
- [13] A. Rezaei, L. Hadian-Dehkordi, H. Samadian, M. Jaymand, H. Targhan, A. Ramazani, H. Adibi, X. Deng, L. Zheng, H. Zheng, *Sci. Rep.* **2021**, *11*, 1.
- [14] A. Rezaei, A. Ramazani, F. Gouranlou, S. Woo Joo, *Lett. Organic Chem.* **2017**, *14*, 86.
- [15] A. Ramazani, F. Z. Nasrabadi, A. Rezaei, M. Rouhani, H. Ahankar, P. A. Asiabi, S. W. Joo, K. Ślepokura, T. Lis, *J. Chem. Sci.* **2015**, *127*, 2269. <https://doi.org/10.1007/s12039-015-0988-6>.
- [16] B. Adibi-Motlagh, A. S. Lotfi, A. Rezaei, E. Hashemi, *Mater. Sci. Eng. C* **2018**, *82*, 323.
- [17] H. Derakhshankhah, R. Jahanban-Esfahlan, S. Vandghanooni, S. Akbari-Nakhjavani, B. Massoumi, B. Haghshenas, A. Rezaei, A. Farnudiyani-Habibi, H. Samadian, M. Jaymand, *J. Appl. Polym. Sci.* **2021**, *138*(24), 50578.
- [18] B. Massoumi, M. Abbasian, B. Khalilzadeh, R. Jahanban-Esfahlan, A. Rezaei, H. Samadian, H. Derakhshankhah, M. Jaymand, *Int. J. Polym. Mater. Polym. Biomater.* **2020**, *1*, 1. <https://doi.org/10.1080/00914037.2020.1760271>.
- [19] H. Derakhshankhah, R. Mohammad-Rezaei, B. Massoumi, M. Abbasian, A. Rezaei, H. Samadian, M. Jaymand, *J. Mater. Sci.* **2020**, *1*, 10947. <https://link.springer.com/article/10.1007/s10854-020-03712-0>.
- [20] M. Sayyed, S. I. Qashou, Z. Khattari, *J. Alloys Compn.* **2017**, *696*, 632.
- [21] A. K. Singh, R. K. Singh, B. Sharma, A. K. Tyagi, *Radiat. Phys. Chem.* **2017**, *138*, 9.
- [22] Q. Li, Y. Wang, X. Xiao, R. Zhong, J. Liao, J. Guo, X. Liao, B. Shi, *J. Hazard. Mater.* **2020**, *398*, 122943. <https://doi.org/10.1016/j.jhazmat.2020.122943>.
- [23] H. Sun, P. J. Sadler, *Metallopharmaceuticals II*, Springer, Berlin, Heidelberg, **1999**, p 159. https://doi.org/10.1007/978-3-642-60061-6_5.
- [24] P. J. Sadler, H. Li, H. Sun, *Coord. Chem. Rev.* **1999**, *185*, 689.
- [25] H. Samadian, H. Mobasheri, S. Hasanpour, J. Ai, M. Azamie, R. Faridi-Majidi, *J. Mol. Liq.* **2020**, *298*, 112021.
- [26] H. Samadian, A. Ehterami, A. Sarrafzadeh, H. Khastar, M. Nikbakht, A. Rezaei, L. Chegini, M. Salehi, *Int. J. Biol. Macromol.* **2020**, *150*, 380.
- [27] B. Massoumi, R. Massoumi, N. Aali, M. Jaymand, *J. Polym. Res.* **2016**, *23*, 136.
- [28] H. Shirkanloo, M. Safari, S. M. Amini, M. Rashidi, *Nanomed. Res. J.* **2017**, *2*, 230.
- [29] M. H. Hazlan, M. Jamil, R. M. Ramli, N. Z. N. Azman, *Appl. Phys. A* **2018**, *124*, 497.
- [30] H. Ji, R. Zhao, N. Zhang, C. Jin, X. Lu, C. Wang, *NPG Asia Mater.* **2018**, *10*, 749.

How to cite this article: Rashidi M, Rezaei A, Bijari S, et al. Microfibers nanocomposite based on polyacrylonitrile fibers/bismuth oxide nanoparticles as X-ray shielding material. *J Appl Polym Sci.* 2021;138:e50755. <https://doi.org/10.1002/app.50755>